UCRL- 86414
PREPRINT

MASTER -811025--5

Laser-Light-Absorption Studies at 1.06μm, 0.53μm, and 0.35μm Wavelengths

F. Ze
E.M. Campbell
R.E. Turner
V. Rupert
K. Manes
D. Phillion
G. Hermes
S. Hildum
P. Lee
G. Tirsell
B. Pruett
H. Kornblum
W. Martin

This paper was prepared for submittal to
American Physical Society
23rd Annual Meeting, October 12-16, 1981
October 1981

Lawrence Livermore Laboratory

MGW

LASER-LIGHT-ABSORPTION STUDIES AT 1.06μm, 0.53μm and 0.35μm WAVELENGTHS*

F. Ze, E. M. Campbell, R. E. Turner, V. Rupert, K. Manes
D. Phillion, G. Hermes, S. Hildum, G. Tirsell, P. Lee, B. Pruett,
H. Kornblum and W. Martin

Lawrence Livermore National Laboratory

October 1981

Abstract

We present the results of light absorption in a series of wavelength scaling experiments recently completed at LLNL. The Argus facility was used to do target studies at 1.06μm, 0.53μm and 0.35μm. Box calorimeter scattered light measurements implied greatly improved laser light absorption for both high Z and low Z plasmas at laser wavelengths shorter that 1.06μm. Furthermore, at the 0.35μm laser wavelength, the inferred absorption is nearly 100% over a substantial range of incident laser intensities. Our results further show a dramatic decrease in the stimulated Brillouin scattered light at 0.35μm relative to the values at 1.06μm and 0.53μm.

---

*Work performed under the auspices of the U. S. Department of Energy by the Lawrence Livermore National Laboratory under contract number W-7405-ENG-48.

Introduction

The Argus laser facility offered great flexibility to experimentally investigate some of the laser-plasma interaction processes which are of fundamental interest to the ICF research program. The absorption of laser light by laser induced plasmas is one of these processes and it is universally agreed that efficient absorption is one of the key factors that ultimately might determine which laser wavelength will be most suitable for a successful ICF program. In this report we show that the use of shorter laser wavelengths greatly improve laser light absorption by both high Z and low Z plasmas.

The experiments were conducted at the Argus laser facility shown schematically in Figure 1. Results of the 1.06μm experiments were obtained before the facility was successively frequency doubled and frequency tripled by the use of the KDP Type 2 crystals shown in the figure. Values of the absorption coefficients were inferred from scattered light measurements by a target-enclosing box calormeter shown in the figure, in conjuction with the incident beam, the tramsmitted beam and the back-reflected beam calorimeters. The combination of the box calorimeter and the focusing and transmission f/2 optics covered 98% of the 4π sr about the target. Complete coverage in the backscattered direction was achieved by slightly reducing the defining hard aperture of the image-relayed[1] laser, resulting in an effective f/2.2 focusing optical system. The box calorimeter panel facing this effective f/2.2 focused beam had an f/2 laser entrance aperture. Other diangostics used during the wavelength scaling experiments are also listed in the figure.

Details of the box calorimeter configuration are shown in Figure 2, which shows a 0.35μm laser beam incident on a gold microdisk enclosed inside the box. The box configuration during the two other wavelength experiments was the same as shown except that the absorber materials were different. The 1.06μm and the 0.53μm series used Schott NG-1 absorber, while a Schott GG-19 absorber was used in the 0.35μm series. Plasma deris were prevented from reaching the absorber by a GW-280 glass shield, as shown in the figure. During the series care was taken to regularly replace plasma shield panels when they became too heavily coated to prevent residual light absorption by the shield.

Another important parameter in laser plasma interaction experiments is the studies of the spectral composition and corresponding intensities of the fraction of light which is not absorbed by the target. This un-absorption light is observed to be mainly backscattered and is the result of stimulated parametric instabilities. Among these both the stimulated Brillouin and Raman instabilites are of major concern to laser fusion research since they scatter substantial factions of incident laser energy away from the target. They are the results of three wave resonant interactions and correspond to the coupling of the laser light wave to the plasma ion accoustic waves and to the plasma electron waves, respectively. The measured scattered light wave frequency is the difference between the incident light wave and the corresponding electrostatic wave frequency. Ion accoustic waves have very low frequencies relative to a light wave, so that they are very dangerous since the scattered light wave will carry most of the three wave interaction energy. But, Raman waves have an additional effect. Since in this instance light waves are coupled to the plasma electron waves, their electric field can sufficiently heat a small fraction of the plasma electrons to suprathermal energies (see Figure 3). For this reason, in fusion experiments using a laser light, an account should be made of the laser light which is not absorbed by the target. We measured the Brillouin backscatter light's during the wavelength scaling series at Argus. In this report it will be shown that the use of shorter laser wavelengths to drive fusion targets can significantly decrease the amount of laser energy converted into this parametric instability.

Experimental Condition

The experimental conditions under which the wavelength scaling experiments were conducted at Argus are listed in Table 1. During the absorption experiments, low Z and high Z microdisks were irradiated at angles of incidence varying between 0^{0} and 45^{0}, with the laser beam diameter at the target plane varying between 80μm and ∿200μm. The irradiance on target was between 3×10^{13} W/cm^2 and ∿1×10^{15} W/cm^2. The beams were p-polarized in all cases.

Experimental Results

1. Wavelength Scaling of Laser Light Absorption by a High Z plasma. In Figure 4 we plot absorption coefficients for gold for the three wavelengths investigated at Argus. The figure shows high absorption for all the wavelengths investigated at low laser intensities (>80% for I $\sim 3\times10^{13}$W/cm^2). But at incident irradiances between 5×10^{13}W/cm$^2 \leq I \leq 10^{15}$W/cm^2, laser wavelengths shorter than 1.06μm greatly improve the absorption.

2. Wavelength scaling of laser light absorption by a low Z plasma. In Figure 5 we show the absorption for a low Z plasma versus the laser irradiance I(W/cm^2). Here again it is seen that laser wavelengths shorter than one micron are more efficiently absorbed, with the UV laser ($3\omega_0$) giving highest absorption values (>90%). Data in Figure 5 as well as those of Figure 4 correspond to incident angles of $\leq 30^0$. These two figures show that for the UV laser, over 90% of the laser light is absorbed as is illustrated in Figure 6. This apparent high absorption at shorter laser wavelengths was one of the reasons why transport studies were undertaken at Argus: to understand how energy is transported from the irradiation region to the regions of the target not directly exposed to laser irradiation.

3. Absorption was found to be mainly collisional. In both Figure 4 and 5 it has been seen that the absorption decreases with increasing intensity for a fixed Z number. In Figure 7 we show the results at 1.06μm for three different Z-numbers. The figure shows that relatively high Z targets absorb laser energy better. This Z-dependence on the measured absorption and the apparent decrease in absorption at higher laser intensities are trends that are consistent with an increased role of collional absorption. But a component of the increased reflection at higher laser intensity could be due to simulated Brillouin backscatter, as was discussed earlier in the introduction.

4. Up to $\theta_{inc}=30^0$, the absorption was found to be basically constant for all the wavelength investigated, at fixed irradiance,

irradiation spot size and incident laser energy. This is illustrated in Figure 8 for data taken at $2\omega_0$ and $3\omega_0$. It is seen that the absorption does not significantly change before $\theta_{inc} \geq 45^0$, for both Au and Be. This means that most of the backscattered light up to $\theta_{inc} = 30^0$, is mainly stimulated Brillouin backscattering. So that a knowledge of this backscattered energy can be used as a reliable measure of the effect of the stimulated Brillouin scatter.

5. The Backscatter Fraction of the Incident Laser Energy was Found to Decrease with Decreasing Laser Wavelength. This is illustrated in Figure 9, which gives the backscatter fraction as a function of the irradiance. The figure shows a dramatic drop of backscatter fraction as the laser wavelength becomes shorter than 1.06μm. It is also seen that backscatter decreases with decreasing laser intensity. These trends are in agreement with Lasnex simulation of the stimulated Brillouin backscatter, as is illustrated in Figure 10. The figure is an illustration of the effect of the so-called Q-factor, on the reflectivity. The higher the Q-factor, the more Brillouin backscatter there is. The effective Q-factor is a linear function of the laser intensity I_L and varies as $\lambda^{7/3}$ at fixed intensity.

6. For Energy Balance Consideration, we found that the fraction of scattered light going into Raman instability was practically negligible at laser wavelengths shorter than 1.06μm, so negligible at $\lambda_L = 0.35\mu m$ that it was lower than the threshold value of the diagnostics in use during the Argus wavelength scaling series.

References

1. J. T. Hunt, J. A Glaze, W. W. Simmons and P. A. Renard, in "Suppression of Self-focusing Through Low-Pass Spatial Filtering and Relay Imaging", Appl. Opt. 17, 2053 (1978).

EXPERIMENTAL LAYOUT FOR WAVELENGTH SCALING EXPERIMENTS

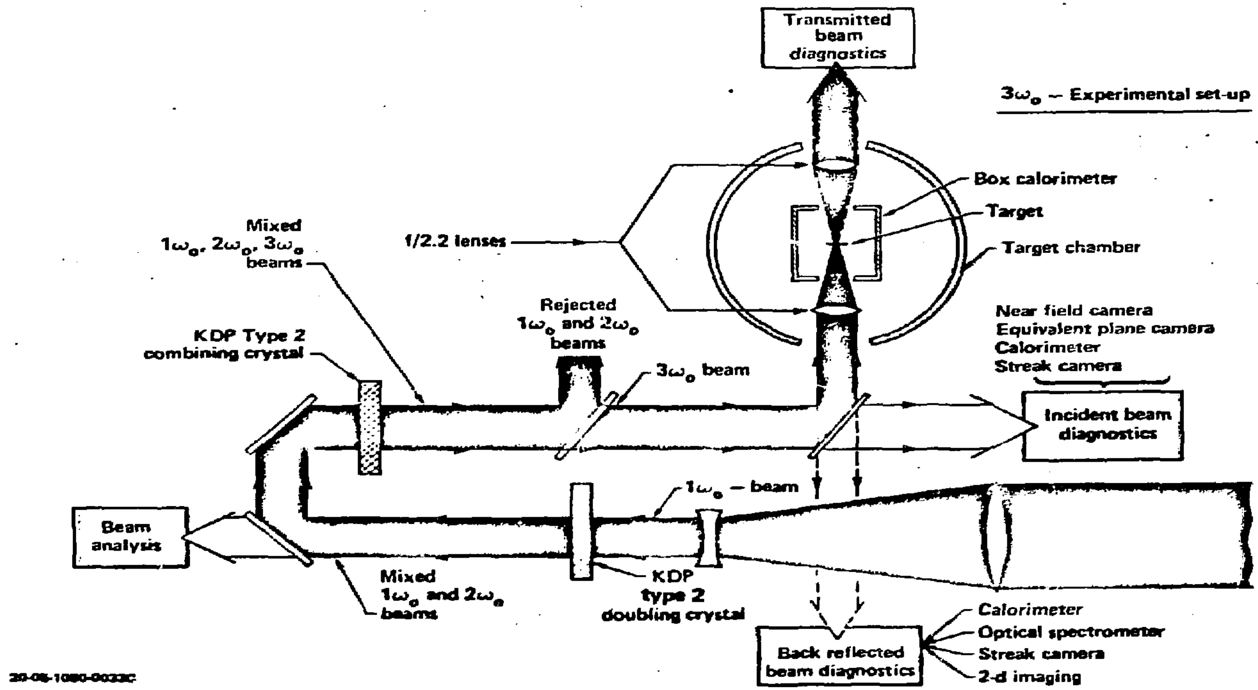

Fig 1

ABSORPTION: TARGET IRRADIATION WAS DONE INSIDE A BOX CALORIMETER TO MEASURE SCATTERED LASER LIGHT DURING ABSORPTION MEASUREMENTS

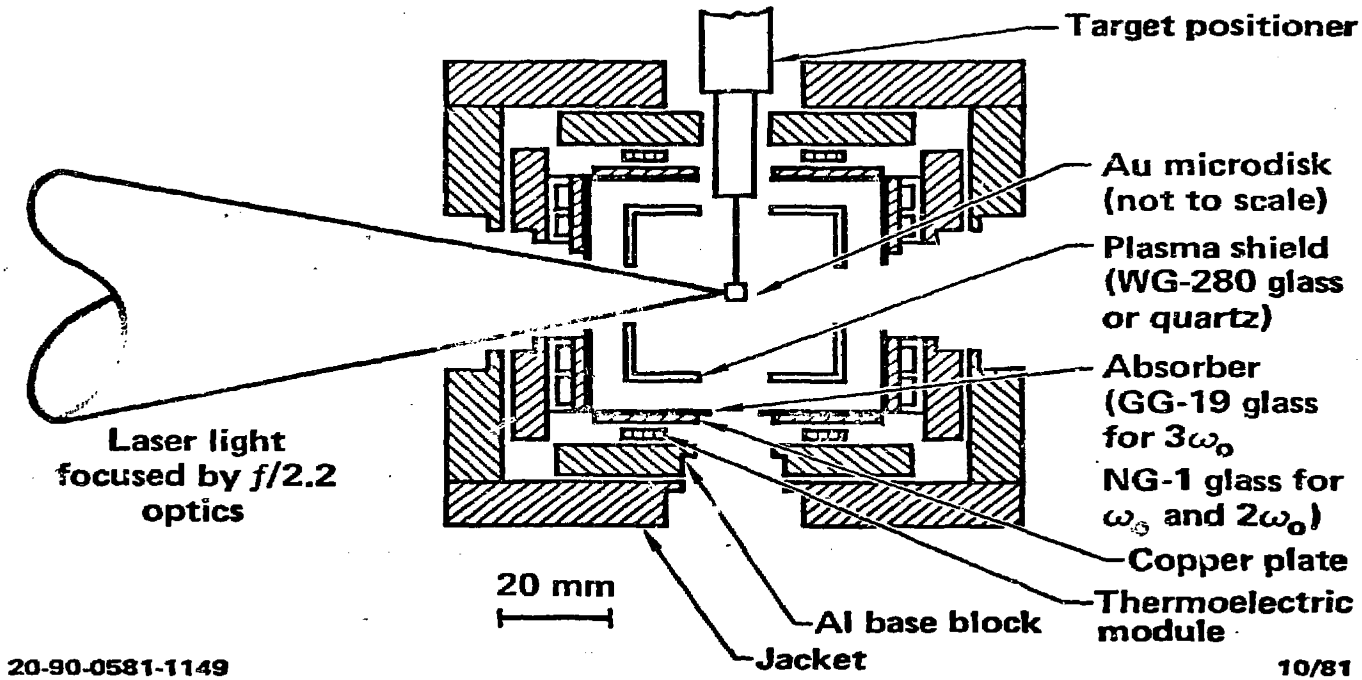

20-90-0581-1149

10/81

Fig 2

MAJOR PLASMA PHYSICS COUPLING PROCESSES

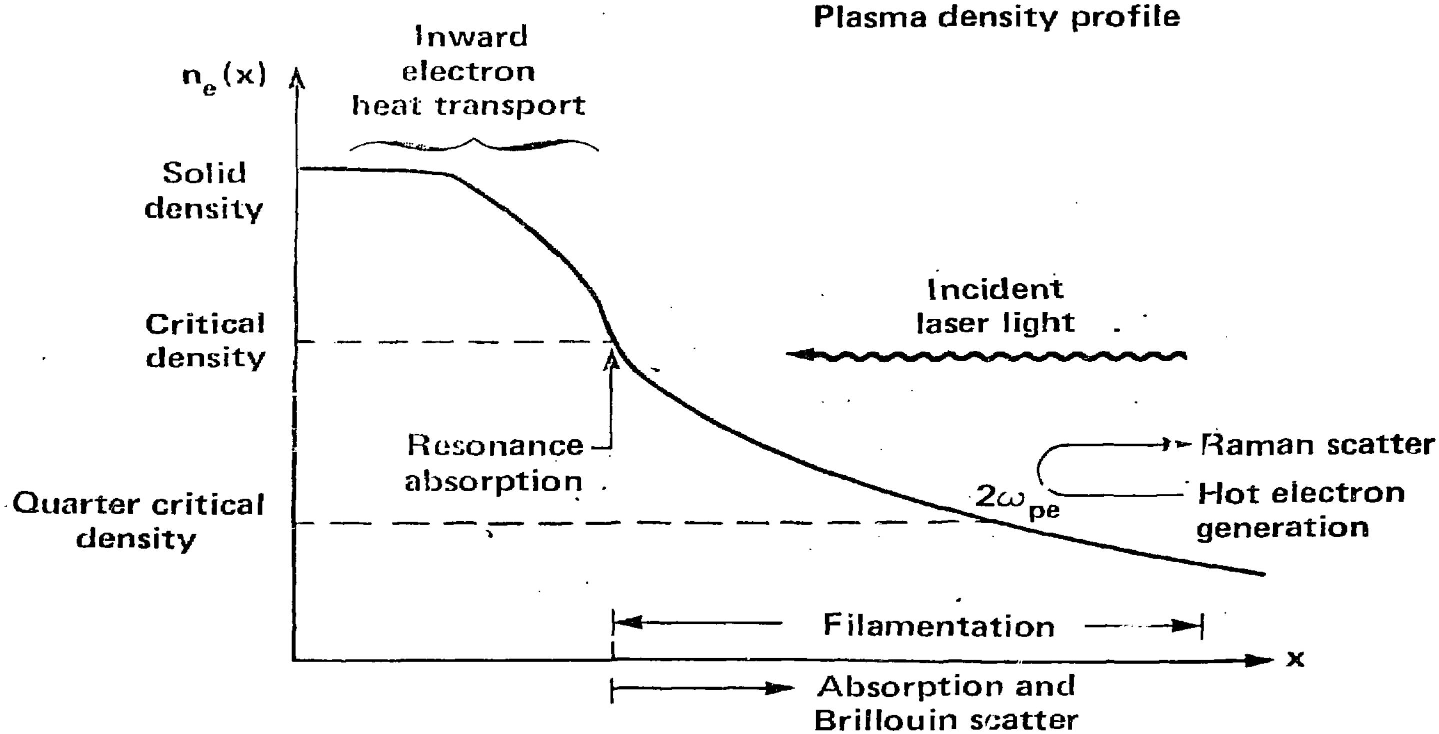

3

$1\omega_o$, $2\omega_o$, AND $3\omega_o$ ABSORPTION — Au DISK TARGETS

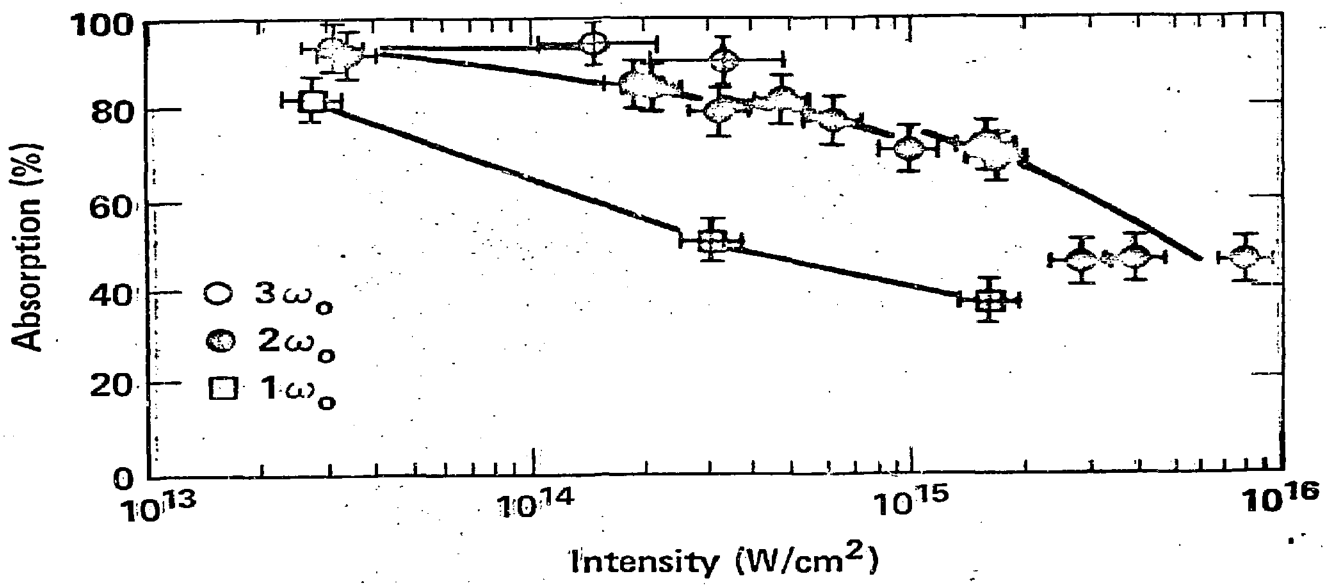

20-90-0381-0677

9/81

Fig. 4

$1\omega_o$, $2\omega_o$, AND $3\omega_o$ ABSORPTION — Be DISK TARGETS

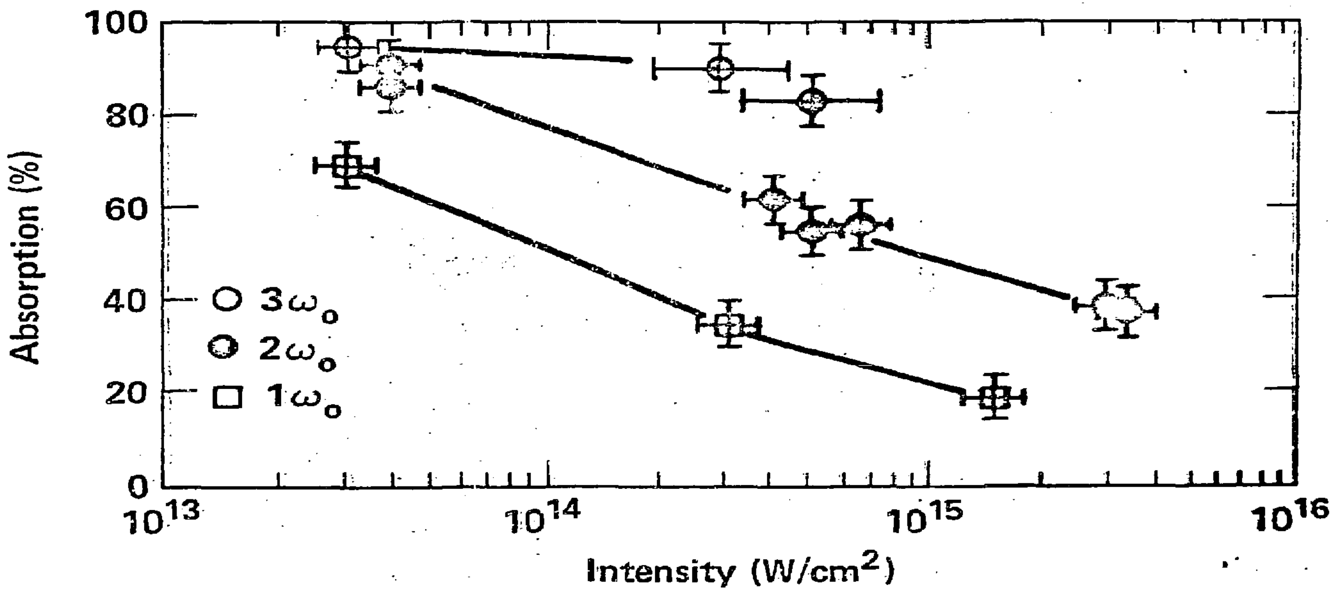

20-90-0381-0676

9/81

Fig. 1

3Wo EXPERIMENTS: ENERGY BALANCE MEASUREMENTS SUGGEST THAT OVER 90% OF THE INCIDENT LASER ENERGY

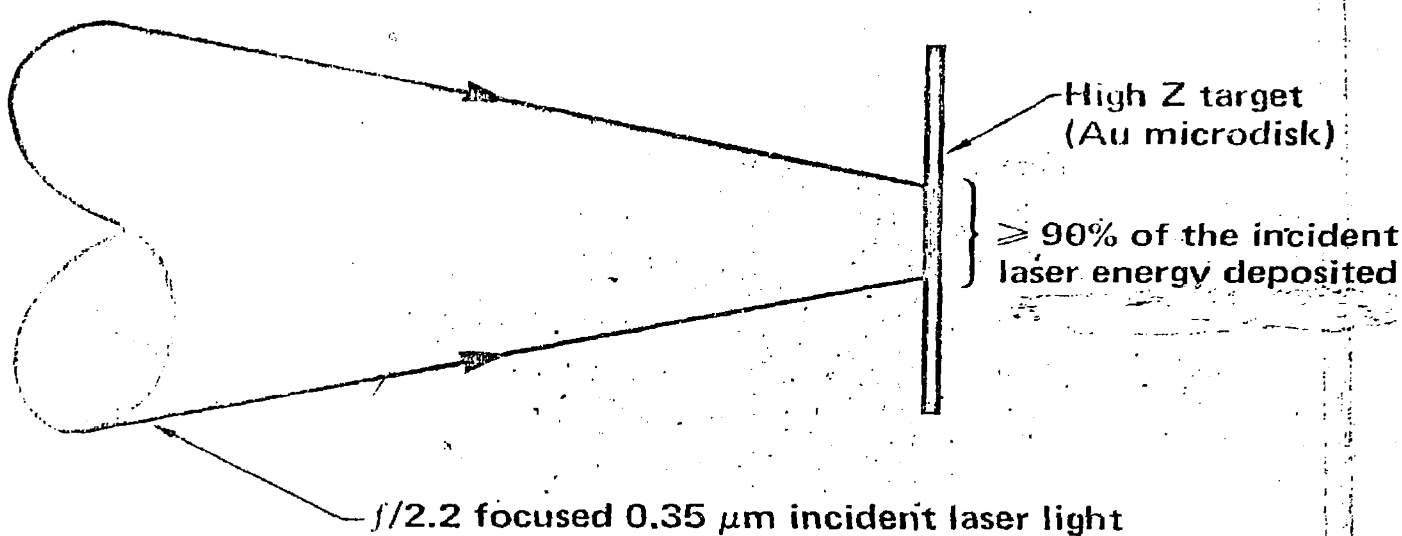

20-90-0581-1147

Fig 6

ABSORPTION OF DISK TARGETS AT 1 μm

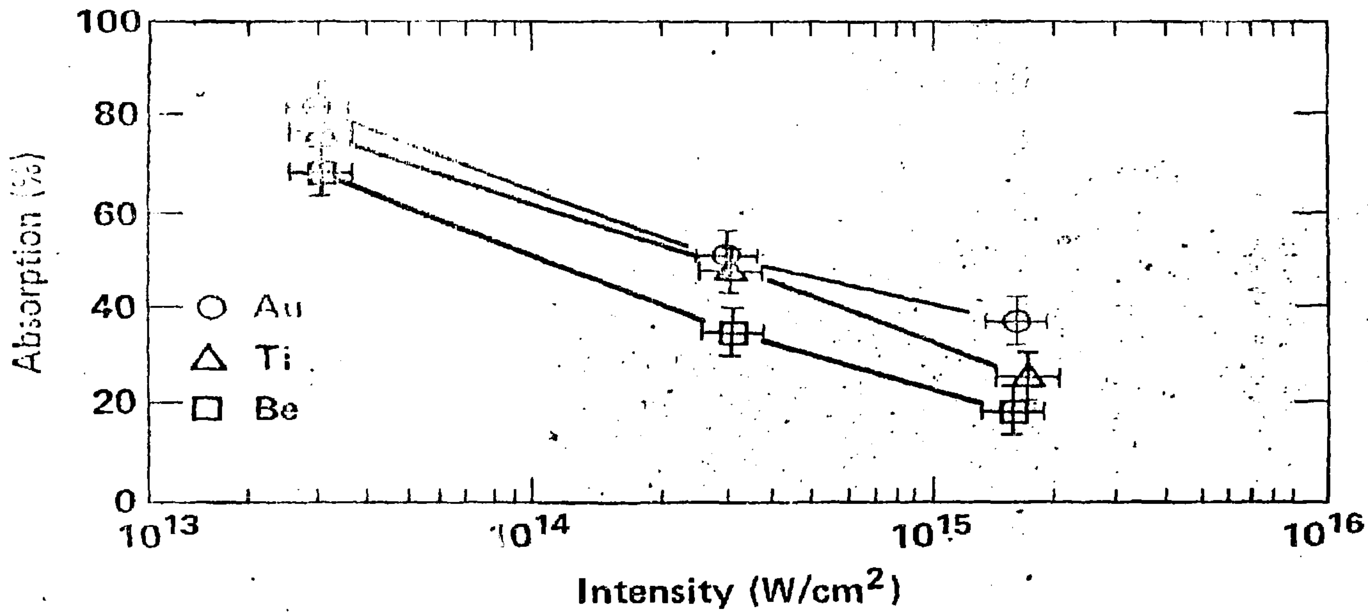

:0-0381-0678

Fig 7

$2\omega_0$ EXPERIMENTS

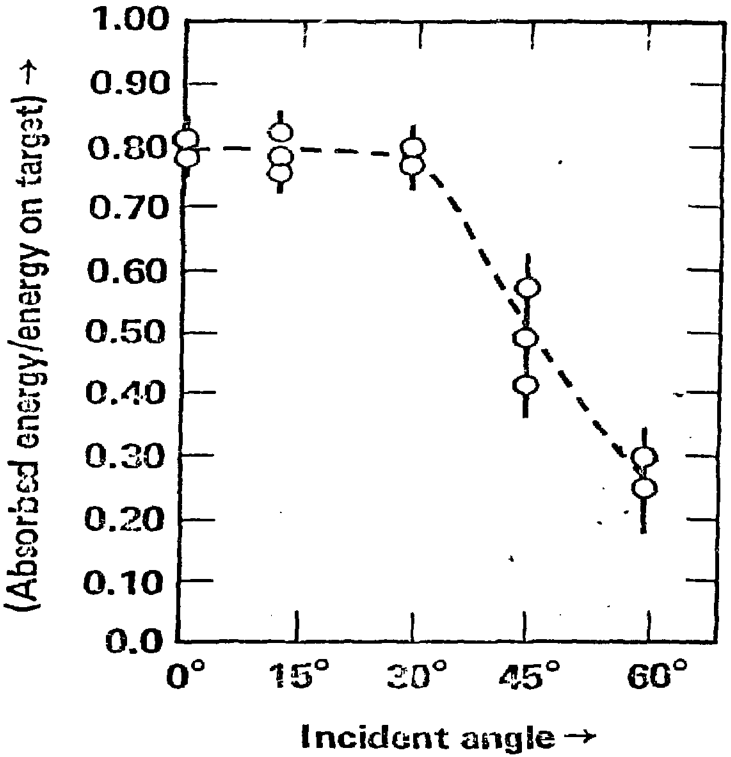

$2\omega_0$ – experiments:

Target: Gold disc

Pulse length τ (ns):

$0.49 \leqslant \tau \leqslant 0.87$

Energy on target E_{inc} (J)

$11.75 \leqslant E_{inc} \leqslant 13$

Irradiance I ($W \cdot cm^{-2}$)

$1 \times 10^{14} \leqslant I \leqslant 3.5 \times 10^{14}$

Focusing lens f/2.2

Fig 8a

20-15-0180-0031

$3\omega_0$ EXPERIMENTS: THE FRACTION OF ABSORBED ENERGY WAS INVESTIGATED FOR ANGLE OF INCIDENCE DEPENDENCE FOR BOTH HIGH AND LOW Z-TARGETS

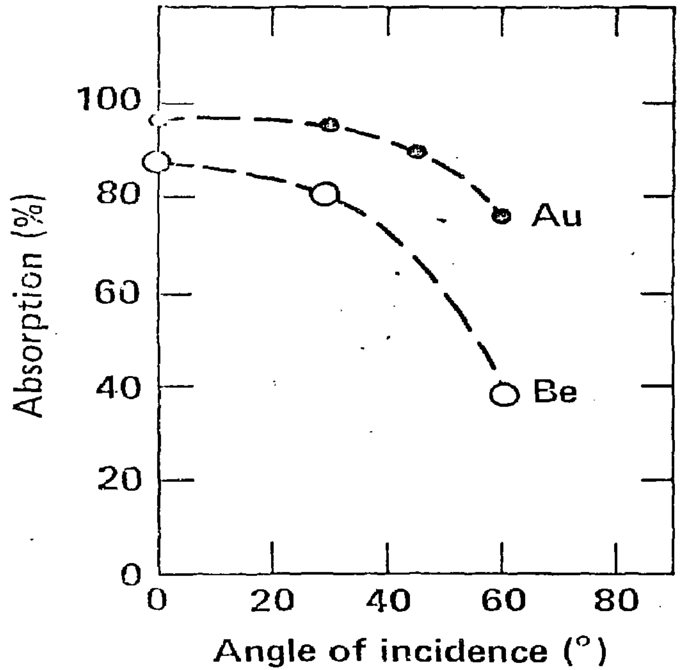

$I_L \sim 2 \times 10^{15}$ W/cm^2

$E_L \sim$ 26–30 J

$\lambda_L = 0.35\ \mu$m

Fig 8 b

20-90-0581-1137

BACKSCATTER FRACTION vs INTENSITY (f/2 COLLECTING LENS)

$\lambda_L = 0.532\ \mu m$

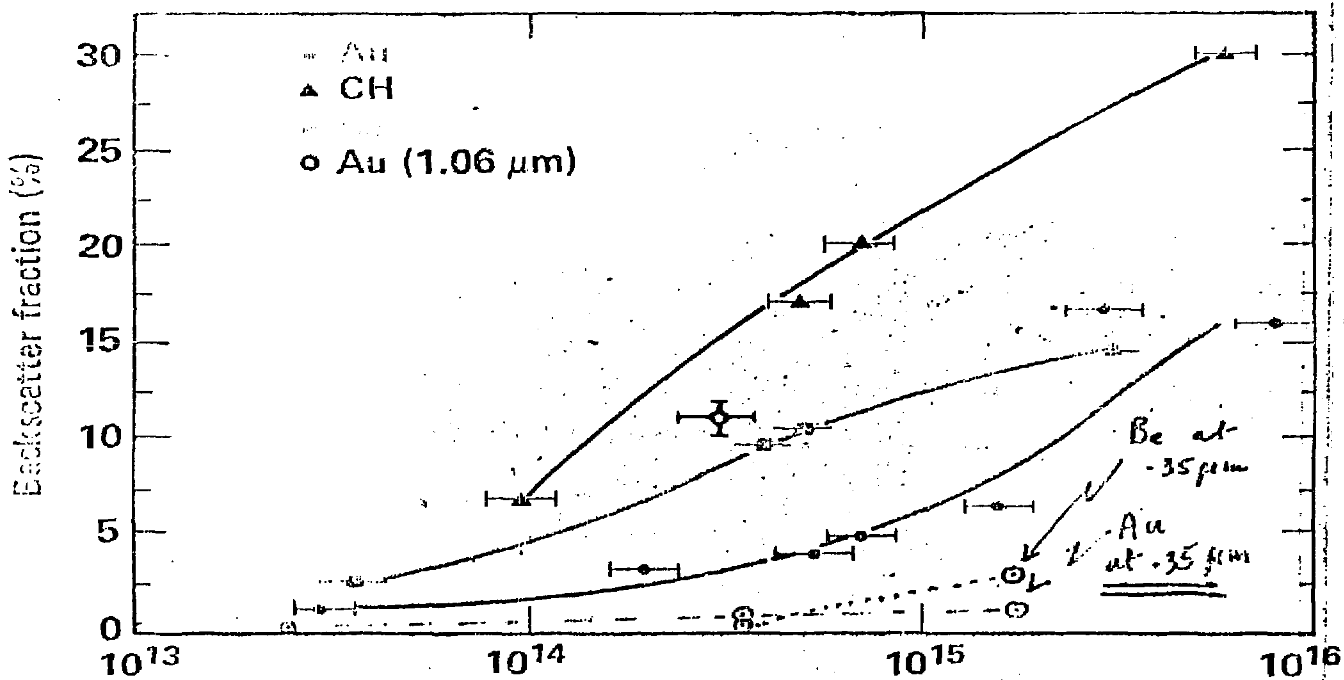

20-90-0580-1637

9/80

Fig 9

IF UNDERDENSE PLASMA IS LARGE, YOU CAN PARAMETRIZE THE AMOUNT OF BRILLOUIN BY A "QUALITY FACTOR" Q

$Q \equiv$ length of plasma ÷ SBS gain length

$$Q = \left(\frac{\pi}{2}\right)\left(\frac{L}{\lambda_L}\right)\left(\frac{n}{n_c}\right)\left(\frac{E_0^2}{8\pi n_c T}\right)$$

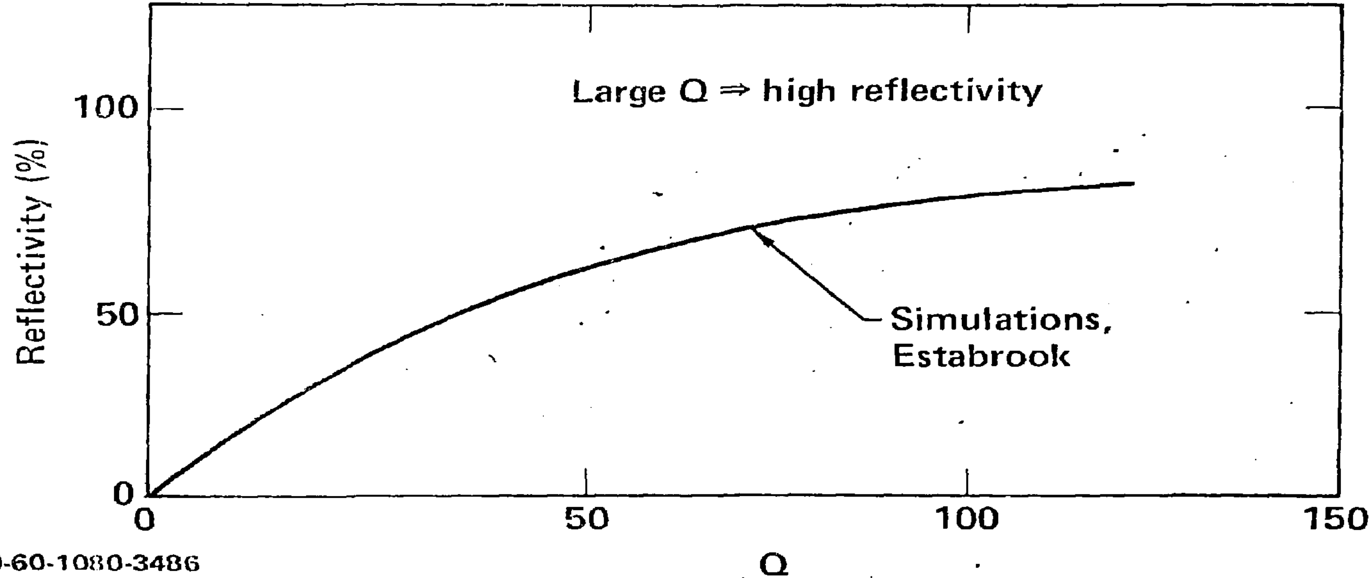

50-60-1080-3486

Fig 10a

WHEN COLLISIONS ARE STRONG, BRILLOUIN CAN BE SHARPLY REDUCED BY USING SHORT WAVELENGTHS

- Consider strong inverse Bremsstrahlung: $L_{abs} < L_n$
- SBS only occurs over a distance $<$ 1 absorption length
- In linear profile $n_e(x) = n_c(x/L_n)$, absorption length is

$$L_{abs} = \left[\frac{3c L_n^2}{\nu_{ei}(n_c)}\right]^{1/3}, \nu_{ei}(n_c) \propto n_c T_e^{-3/2}$$

- Quality factor for SBS:

$$Q_{eff} \cong \frac{\pi}{2}\left(\frac{E_o^2}{8\pi n_c T_e}\right)\int_{x=0}^{L_{abs}}\left(\frac{x}{L_n}\right)\frac{dx}{\lambda_L}$$

$$\boxed{Q_{eff} \propto \frac{I_L \lambda_L^{7/3}}{L_n}, \text{ linear profile}}$$

(For uniform plasma, $Q_{eff} \propto \lambda_L^{11/3}$)

50-60-1080-3484